

Linköping University Postprint

Near-edge x-ray absorption studies of Na-doped tetracyanoethylene films: A model system for the $V(\text{TCNE})_x$ room-temperature molecular magnet

E. Carlegrim, B. Gao, A. Kanciurzevska, M. P. de Jong, Z. Wu, Y. Luo and M. Fahlman

N.B.: When citing this work, cite the original article.

Original publication:

E. Carlegrim, B. Gao, A. Kanciurzevska, M. P. de Jong, Z. Wu, Y. Luo and M. Fahlman, Near-edge x-ray absorption studies of Na-doped tetracyanoethylene films: A model system for the $V(\text{TCNE})_x$ room-temperature molecular magnet, 2008, Physical Review B, (77), 054420.

<http://dx.doi.org/10.1103/PhysRevB.77.054420>.

Copyright: The America Physical Society, <http://prb.aps.org/>

Postprint available free at:

Linköping University E-Press: <http://urn.kb.se/resolve?urn=urn:nbn:se:liu:diva-11753>

Near-edge x-ray absorption studies of Na-doped tetracyanoethylene films: A model system for the $V(\text{TCNE})_x$ room-temperature molecular magnet

E. Carlegrim,¹ B. Gao,^{2,3} A. Kanciużewska,¹ M. P. de Jong,⁴ Z. Wu,³ Y. Luo,² and M. Fahlman¹

¹Department of Science and Technology (ITN), Linköping University, S-601 74 Norrköping, Sweden

²Department of Theoretical Chemistry, School of Biotechnology, Royal Institute of Technology, SE-10691 Stockholm, Sweden

³Institute of High Energy Physics, Chinese Academy of Sciences, Beijing 100049, China

⁴Department of Physics, Chemistry and Biology (IFM), Linköping University, S-581 83 Linköping, Sweden

(Received 22 May 2007; revised manuscript received 15 November 2007; published 19 February 2008)

$V(\text{TCNE})_x$, with $\text{TCNE}=\text{tetracyanoethylene}$ and $x\sim 2$, is an organic-based molecular magnet with potential to be used in spintronic devices. With the aim of shedding light on the unoccupied frontier electronic structure of $V(\text{TCNE})_x$ we have studied pristine TCNE and sodium-intercalated TCNE by near edge x-ray absorption fine structure (NEXAFS) spectroscopy as well as with theoretical calculations. Sodium-intercalated TCNE was used as a model system of the more complex $V(\text{TCNE})_x$ and both experimental and theoretical results of the model compound have been used to interpret the NEXAFS spectra of $V(\text{TCNE})_x$. By comparing the experimental and theoretical C K -edge of pristine TCNE, the contributions from the various carbon species (cyano and vinyl) could be disentangled. Upon fully sodium intercalation, TCNE is n doped with one electron per molecule and the features in the C and N K -edge spectra of pristine TCNE undergo strong modification caused by partially filling the TCNE lowest unoccupied molecular orbital (LUMO). When comparing the C and N K -edge NEXAFS spectra of fully sodium-doped TCNE with $V(\text{TCNE})_x$, the spectra are similar except for broadening of the features which originates from structural disorder of the $V(\text{TCNE})_x$ films. The combined results from the model system and $V(\text{TCNE})_x$ suggest that the lowest unoccupied molecular orbital with density on the nitrogen atoms in $V(\text{TCNE})_x$ has no significant hybridization with vanadium and is similar to the so-called singly occupied molecular orbital of the TCNE anion. This suggests that the LUMO of $V(\text{TCNE})_x$ is TCNE^- or vanadiumlike, in contrast to the frontier occupied electronic structure where the highest occupied molecular orbital is a hybridization between $V(3d)$ and cyano carbons. The completely different nature of the unoccupied and occupied frontier electronic structure of the material will most likely affect both charge injection and transport properties of a spintronic device featuring $V(\text{TCNE})_x$.

DOI: [10.1103/PhysRevB.77.054420](https://doi.org/10.1103/PhysRevB.77.054420)

PACS number(s): 75.50.Xx, 73.61.Ph, 71.15.Mb

INTRODUCTION

In the growing field of spintronics (spin-based electronics),^{1,2} there is a strong need for development of flexible light-weight magnets.³ Organic-based magnets are attractive candidates since they are so-called “designer magnets,” which means that their properties are possible to tune by organic chemistry. $V(\text{TCNE})_x$, $x\sim 2$, belongs to one of these organic-based magnetic systems $M(\text{TCNE})_x$ (M stands for metal, $M=\text{V}$, Mn , Fe , etc., $\text{TCNE}=\text{tetracyanoethylene}$)⁴⁻⁷ and is particularly interesting since it is a semiconductor and has a Curie temperature well above room temperature.^{4,8}

Until recently, the occupied electronic structure of $V(\text{TCNE})_x$ was not known, mainly because of its extreme air sensitivity and therefore difficulties of performing measurements of the compound. By means of a *in situ* deposition method, we solved the oxidation problems and characterized the electronic and magnetic properties of ultrathin $V(\text{TCNE})_x$ films using photoelectron spectroscopy (PES), resonant photoemission, x-ray absorption spectroscopy (XAS), and x-ray magnetic circular dichroism (XMCD).⁹ However, due to the lack of knowledge regarding the physical structure of the compound,¹⁰ it is impossible to perform accurate theoretical calculations of the ground-state electronic structure that would be extremely valuable for the interpretation of the PES and x-ray absorption data. One way

to circumvent this problem is to study the organic building block, TCNE, of $V(\text{TCNE})_x$. Alkali-doped TCNE can serve as a useful model system for the more complex $V(\text{TCNE})_x$ organic-based magnet, as the occupied and unoccupied electronic structures of TCNE and alkali-doped TCNE can be calculated with great accuracy using modern theoretical techniques. We have previously published a study of the occupied electronic structure of rubidium-doped TCNE,¹¹ which provided useful information on the strength of the on-site Coulomb interaction. TCNE was stepwise doped by rubidium and studied by both experimental and theoretical methods in order to reveal the occupied electronic structure of the molecular anion, information that then was used in interpreting the photoelectron spectroscopy results on the occupied electronic structure of *in situ* grown $V(\text{TCNE})_x$ films.⁹ The combined results can be summarized as follows. The TCNE moieties of Rb-doped TCNE and $V(\text{TCNE})_x$ carry about one negative charge each, yielding mainly $V^{2+}(\text{TCNE})_2^-$ in the $V(\text{TCNE})_x$ films and Rb^+TCNE^- in the Rb-doped films.^{9,11} In contrast to the ionic charge transfer complex, Rb^+TCNE^- , there is a more covalent bonding character between the vanadium and the TCNE molecules, involving significant hybridization between the occupied $V(3d)$ and the frontier occupied π -electronic states of the TCNE.^{9,12} PES in combination with RPE measurements of $V(\text{TCNE})_x$ shows that the highest occupied state at 1 eV has strong $V(3d)$ character while the next two discernible occu-

pied frontier states at 2.5 and 3.5 eV mainly are derived from orbitals localized on $(\text{TCNE})^-$.⁹ The nature and origin of the unoccupied electronic structure of $\text{V}(\text{TCNE})_x$ remains a mystery, however, as theoretical modeling of the $\text{V}(\text{TCNE})_x$ C and N *K*-edge x-ray absorption spectra are not possible due to the lack of information on the physical structure of the compound as mentioned previously.¹⁰ It should be pointed out that the V *L*-edge case is quite different, due to the strong interaction between the $2p$ core holes and the $3d$ valence electrons, which confines the core-excited states on the V ions. Consequently, the *L*-edge XAS/XMCD spectra reflect the atomic multiplet structure, which is only dependent on the local environment of the vanadium ion, enabling interpretation of the data using ligand field- and charge transfer multiplet calculations.¹² However, these previous studies have not addressed the nature of the unoccupied density of states, which is of key importance in spintronic devices as it influences electron injection and electron transport properties of the material. The aim of this present study is hence to model the unoccupied density of states of $\text{V}(\text{TCNE})_x$, using Na-doped TCNE as a model system following the successful approach demonstrated for the occupied electronic structure.^{9,11,12}

The nature of the unoccupied electronic structure of TCNE and how it changes upon the addition of a charge also is of interest to so-called molecule-based electronics where a single molecule can form the active part of a transistor.^{13,14} Unlike the case for large molecules and polymers where doping leads to charged states (polarons and bipolarons) with relatively large extensions and small relaxation energies,^{15–17} charge localization and Coulomb interactions are significant in small organic molecules such as TCNE (Refs. 11 and 18) and hence are important for both charge injection and transport in molecular-based devices. Indeed, the above mentioned study of rubidium-intercalated TCNE shows that on-site Coulomb-interaction (strength ~ 2 eV) prevents the formation of doubly charged TCNE regardless of doping level and results in the formation of a Coulomb gap around the Fermi level upon doping.¹¹

The molecular structure of TCNE and TCNE^- ,¹⁹ as well as the vertical excitation energies of TCNE and TCNE^- for low energy transition (< 10 eV),^{20,21} have been studied theoretically. For TCNE, the lowest singlet excited state involves promotion from the highest occupied molecular orbital (HOMO) into the lowest unoccupied molecular orbital (LUMO).^{20,21} The TCNE is reduced into its anion TCNE^- , the former LUMO becomes singly occupied forming a so-called singly occupied molecular orbital (SOMO).^{11,19,21} This affects the excitation energies and for TCNE^- the lowest energy excitation is formed by promotion of an electron from the previous HOMO into the singly occupied molecular orbital.²¹

In this paper, we present a combination of experimental and theoretical results that give information about the unoccupied levels in TCNE and at which part of the molecule they are localized. Sodium-doped thin films of TCNE have been prepared and characterized with PES, near edge x-ray absorption fine structure (NEXAFS) and theoretical calculations. The emphasis in this study is on the NEXAFS part,

since the occupied electronic structure of TCNE, $(\text{TCNE})^-$, and $\text{V}(\text{TCNE})_x$ has been clarified by the recent studies mentioned.^{9,11,12} The experimental and theoretical NEXAFS results on $(\text{TCNE})^-$ and NaTCNE are used to interpret the $\text{V}(\text{TCNE})_x$ NEXAFS data obtained from films deposited by the recently developed technique for *in situ* preparation of oxygen-free films based on chemical vapor deposition (CVD).⁹

EXPERIMENTAL DETAILS

Thin TCNE films were prepared on argon sputter-cleaned gold substrates at a temperature of -130 °C. TCNE was introduced to the vacuum chamber via an external gas handling system. The pressure during deposition was better than 5×10^{-8} mbar, and the base pressure in the chamber was 10^{-10} mbar. Na doping was done *in situ* at 10^{-9} mbar and -130 °C, using an alkali metal source provided from SAES. The sodium was deposited in small steps in order to study the first changes in detail, then the deposition rate was increased. Thin films of $\text{V}(\text{TCNE})_x$ were prepared *in situ* by codeposition of $\text{V}(\text{C}_6\text{H}_6)_2$ and TCNE on argon sputter-cleaned gold substrates at room temperature, using a custom-built UHV-compatible deposition source based on CVD technique.

The films were studied *in situ* using PES and NEXAFS at beamline I311 of the MAX-II storage ring at the synchrotron facility MAX-lab in Lund, Sweden. Additional PES measurements were performed using a spectrometer of our own design. The thin films of TCNE and $\text{V}(\text{TCNE})_x$ were prepared under the same conditions in MAX-lab as in the home laboratory. The I311 end-station is equipped with a Scienta SES-200 electron energy analyzer and the base pressure of the system during the measurements was in the low 10^{-9} mbar range. NEXAFS measurements were performed using the partial electron yield method. The energy calibration was performed such that errors of the monochromator and the analyzer were taken into consideration. In order to remove the background, all NEXAFS spectra were divided by a reference spectrum of sputter-cleaned gold, taken at the C *K* edge, N *K* edge, and V *L* edge, respectively. A substantial “carbon dip” was present for the C *K*-edge NEXAFS spectra, which makes the background subtraction significantly less accurate and complicates comparison between experiment and theory for these spectra. The PES and NEXAFS of the NaTCNE films were carried out at -130 °C, and at RT for $\text{V}(\text{TCNE})_x$.

THEORETICAL METHODOLOGY

The geometry of tetracyanoethylene (TCNE, C_6N_4), its anion $(\text{TCNE})^-$, and doped compound NaTCNE were optimized at the (unrestricted) B3LYP/6-31G* level. The gradient-corrected Becke (BE88) exchange functional and the Perdew (PD86) correlation functional were used to calculate the NEXAFS spectra of the carbon and nitrogen atoms using the so-called Δ Kohn-Sham (Δ KS) scheme, wherein the energy of a particular x-ray absorption transition is obtained as the difference between the energy of the excited

state and that of the ground state. The orbital basis set used for the carbon/nitrogen atom was a triple- ζ valence and had the following forms: (7111/411/1) for TCNE and (6321/411/1) for the sodium atom. The IGLO-III basis set of Kutzelnigg, Fleischer, and Shindler was used for the excited carbon/nitrogen atom. A four/five-electron effective core potential (ECP) was used to describe the other carbons/nitrogens. The use of ECP's helps the convergence of the core-hole state and has negligible effects on the accuracy of the calculated spectra. The intensity of the theoretical spectra were calculated using Slater transition potential method in combination with a double basis set technique, where a normal orbital basis set was used in the minimization of the energy, and an added augmented diffuse basis set (19s, 19p, 19d) was used for the excited carbon/nitrogen to obtain better representation of relaxation effects. A Gaussian function [full width at half maximum (FWHM)=0.5 eV] was used for convoluting the spectra below the ionization potential (IP), while a Stieltjes imaging approach^{22,23} was used to describe the spectra above the IP in the continuum. The Gaussian broadening was chosen to simulate the experimental spectra, where the major sources of energy broadening are Gaussian in nature (solid film+light profile from monochromator and slits). Two fundamentally different doping positions were tried, but only the one in best agreement with the experimental data is shown in this paper. Each calculated spectrum was calibrated by shifting it to match each calculated 1s to LUMO transition energy obtained from Δ KS approach by computing specifically the energy difference between the ground state and the relaxed core-excited state. The ionization potential of each 1s orbital was also calculated with Δ -KS scheme where the energy is taken as the difference between the ground state and the fully optimized core-ionized state. The individual NEXAFS contributions plotted for different C and N atoms do not take into account the multiplicity of the atoms in the TCNE molecule, but the overall C and N K-edge theoretical NEXFAS spectra take the multiplicity into account.

RESULTS

The pristine and Na-doped films were studied using PES, with particular emphasis on the N(1s) and C(1s) core levels and the valence electronic region. The evolution of the N(1s) and C(1s) core level spectra as well as the valence region of sodium-doped TCNE was in agreement with the expected results for pristine-to-fully alkali-doped TCNE films.¹¹ The C(1s) and N(1s) core level peaks of TCNE are shifted to 286.5 and 398.8 eV, respectively, for fully sodium-doped system (1 Na per TCNE), see Figs. 1(a) and 1(b). The positions of the core levels of sodium-doped TCNE are in agreement with the main peaks of the corresponding core level spectra of V(TCNE)_x, as was the case for Rb-doped TCNE, which has been used to assign the charge of the TCNE moieties of V(TCNE)_x as being approximately one electron.¹² The valence region of TCNE, Fig. 1(c), undergoes modification upon sodium doping such that in the previously forbidden band gap two new peaks appeared originating from the destabilized highest occupied molecular orbital (HOMO) and

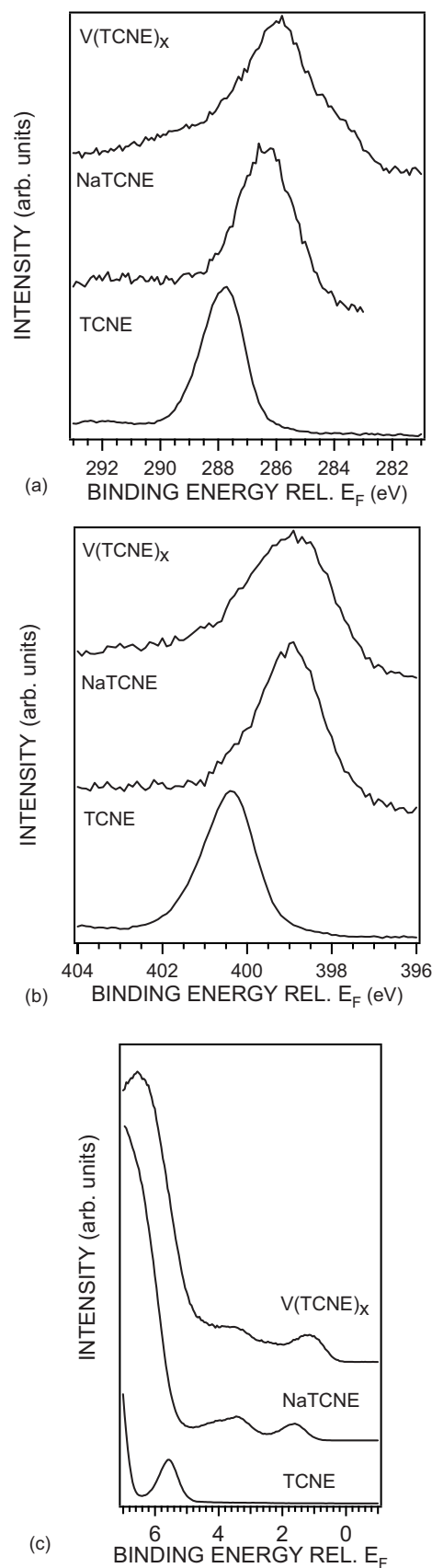
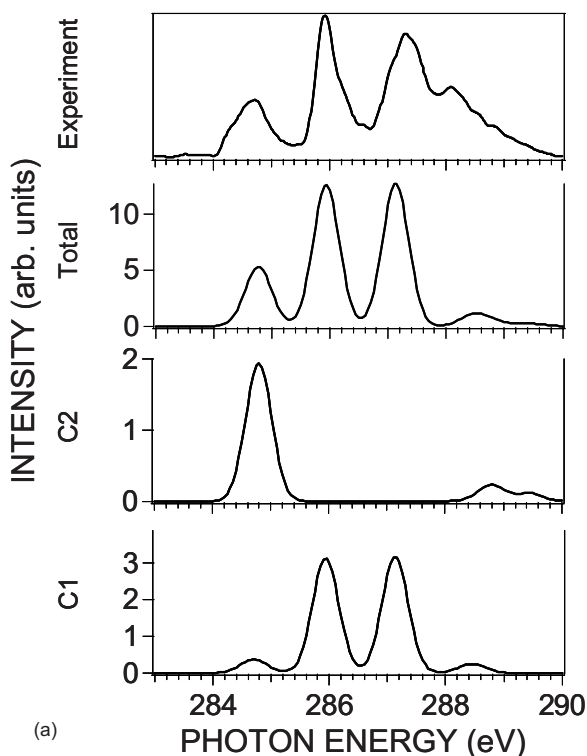
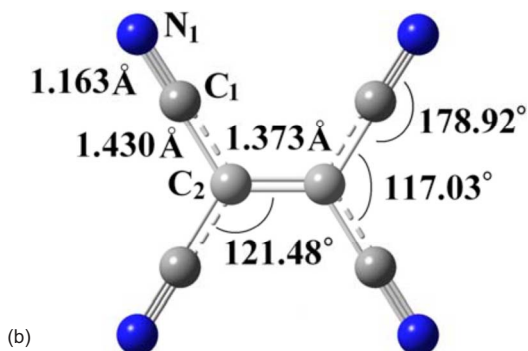


FIG. 1. Photoelectron spectroscopy spectra of (a) the C(1s) core level and (b) the N(1s) core level and (c) the valence region of TCNE, sodium-doped TCNE and V(TCNE)_x.



(a)



(b)

FIG. 2. (Color online) (a) Experimental and calculated C *K*-edge NEXAFS spectra of pristine TCNE. The contributions from the various carbon species (C1: cyano, C2: vinyl) to the overall C *K*-edge NEXAFS spectrum are shown in the bottom two spectra. (b) The optimized structure of TCNE. The calculated lowest ionization potential is 293.4 eV.

the singly occupied molecular orbital (SOMO).¹¹ The frontier valence region of $V(\text{TCNE})_x$ differs from the sodium-doped TCNE case, however, due to the covalent bonding between the vanadium and cyano groups that produces significant hybridization of the HOMO.^{9,12}

In the experimental C *K*-edge NEXAFS spectrum of pristine TCNE three main absorption peaks are visible, see top spectrum, Fig. 2(a). The first peak situated at 284.7 eV has a weak shoulder on the low photon energy side and a second narrow peak is located at 285.9 eV. The third main peak is at 287.3 eV and has a well defined high photon energy shoulder. To shed light on the origin of these NEXAFS features we turn to theoretically derived C *K*-edge NEXAFS spectra displayed in Fig. 2(a). The contributions from the various

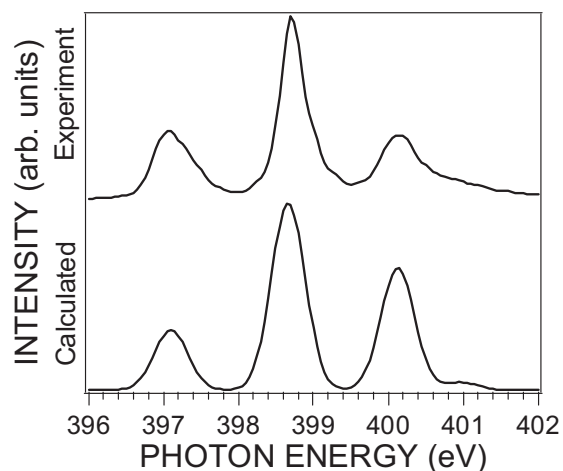
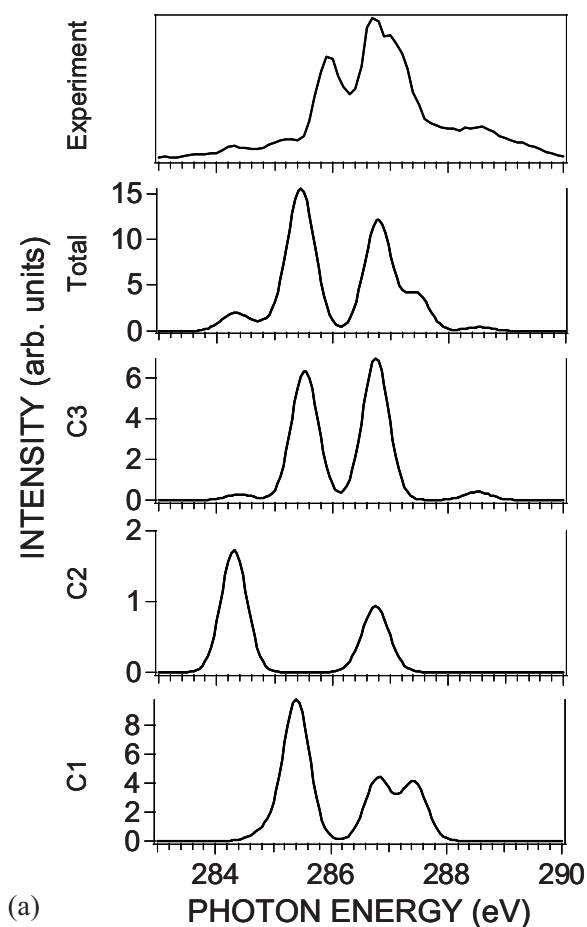


FIG. 3. Experimental and calculated N *K*-edge NEXAFS spectra of pristine TCNE. The calculated ionization potential is 406.0 eV.

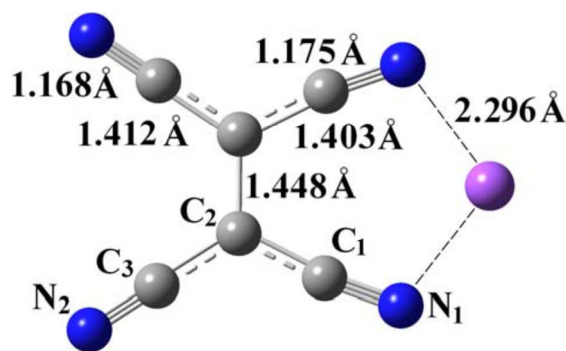
carbon species [C1: cyano, C2: vinyl, see Fig. 2(b)] to the overall C *K*-edge NEXAFS spectrum are shown in the bottom two spectra in the figure. The small shoulder (broadening) towards lower photon energy of the first absorption peak is qualitatively reproduced, as are the following two peaks including the high photon energy shoulder. The first peak is at 284.7 eV with the next two peaks appear at slightly higher photon energies but with differences in relative intensity compared to the experimental C *K*-edge spectrum. The first absorption peak contains contribution from both cyano and vinyl carbon, with the vinyl contribution having a larger weight as can be seen from the relative intensities of the absorption, even when taking into account the differing multiplicities (2 for vinyl vs 4 cyano carbon). The next two absorption peaks, related to the LUMO+1 and LUMO+2, respectively, are almost exclusively derived from the cyano carbons, i.e., the core hole is located on such sites. The feature in the theoretical spectrum that is located in the energy region of the broad high photon energy shoulder of the third peak in the experimental spectrum is related to LUMO+3 and has contributions both from the vinyl and cyano carbons.

The experimental N *K*-edge spectrum of pristine TCNE has been published previously, but we present it here for the convenience of the reader together with the calculated spectrum, see Fig. 3. The first absorption peak is located at 397.1 eV and corresponds to excitation into the LUMO according to the calculated spectra. The second, more narrow, peak in the experimental spectrum with a maximum at 398.7 eV has a corresponding feature in the theoretically derived spectrum, where the absorption event originates from excitation into LUMO+1. The third peak at 400.2 eV in the experimental spectrum also is reproduced by theory, where it is related to excitation into LUMO+2.

In Fig. 4(a) top spectrum we display the experimental C *K*-edge NEXAFS spectrum of fully sodium-doped TCNE (~ 1 Na per 1 TCNE). The strong LUMO feature at 284.7 eV in the pristine TCNE films is replaced by two weak features centered at 284.3 and 285.2 eV. The two peaks at higher energy (285.9 and 287.3 eV) in the pristine C *K*-edge spectrum also undergo strong modification upon doping. The fea-



(a)



(b)

FIG. 4. (Color online) (a) Experimental C *K*-edge NEXAFS spectra of fully sodium-doped TCNE (~ 1 Na per 1 TCNE) and the calculated spectra of NaTCNE. The contributions from the various carbon species [C1 and C3: cyano, C2: vinyl, see Fig. 3(b)] to the overall C *K*-edge NEXAFS spectrum are shown in the bottom three spectra. (b) The optimized structure of NaTCNE. The calculated lowest ionization potential is 287.8 eV.

ture at 285.9 eV significantly drops in relative intensity and instead of a peak at 287.3 eV (pristine TCNE) a double feature 286.7 eV appears with a shoulder at 286.9 eV. The high energy shoulder beyond 288 eV in the pristine spectrum remains, but decreases somewhat in relative intensity upon doping.

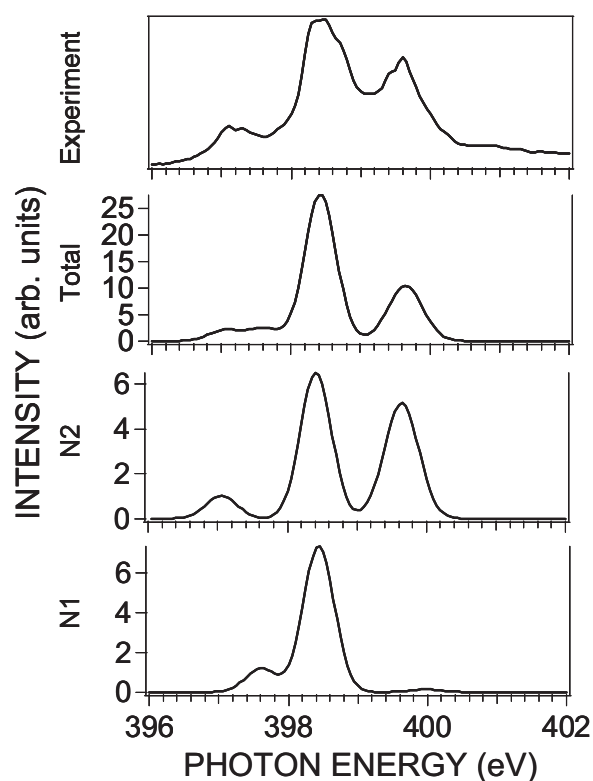


FIG. 5. Experimental N *K*-edge NEXAFS spectra of fully sodium-doped TCNE (~ 1 Na per 1 TCNE) and the calculated spectra of NaTCNE. The contributions from the various nitrogen species [N1, N2, see Fig. 3(b)] to the overall N *K*-edge NEXAFS spectrum are shown in the bottom two spectra. The calculated lowest ionization potential is 400.2 eV.

The other spectra depicted in Fig. 4(a) are theoretically derived C *K*-edge NEXAFS spectra of NaTCNE, with the individual contributions from the different carbon atoms presented as well. We see that the lowest absorption peak (excitation into the now half-filled LUMO) is broadened due to two different contributions where the core hole is located on the C2 and C3 carbons, respectively, see Fig. 4(b). The onset of absorption involves a core hole being created on the C2 carbon (vinyl), which also is the dominant contribution to the frontier absorption peak. The second main peak of the theoretical C *K*-edge NEXAFS spectrum is a peak located at 285.4 eV, resulting from absorption events where excitation into LUMO+1 occurs and the core hole resides on the C1 and C3 carbons. A third peak with a high photon energy shoulder is located at 286.8 eV and is mainly derived from excitation into LUMO+2 and LUMO+3 from C1, C2, and C3 carbons.

In Fig. 5, top spectrum, the experimental N *K*-edge NEXAFS spectrum of fully sodium-doped TCNE is depicted together with the calculated N *K*-edge NEXAFS spectra of NaTCNE, including the individual contributions from the different nitrogen atoms [see Fig. 4(b)]. As for the C *K*-edge case, there is significant modification of the experimental NEXAFS spectrum resulting from the Na doping and partial filling of the LUMO with the LUMO feature at 397.1 eV in the pristine TCNE films decreases in intensity. The main peak at 398.7 eV for pristine TCNE is shifted towards lower

energy ~ 398.4 eV, and a weak shoulder appears on the low photon energy side at ~ 397.8 eV. The absorption peak at 400.2 eV in the pristine N *K*-edge spectrum shifts towards lower photon energies 399.6 eV and increases in relative intensity.

In the calculated N *K*-edge spectrum of NEXAFS spectrum of NaTCNE, the onset of absorption occurs by the creation of a core hole on the cyano nitrogen not coordinated to the sodium [N2, Fig. 4(b)] and excitation of the electron into the partially filled LUMO. A second low intensity feature is located at ~ 397.6 eV and involves excitation into partially filled LUMO and a core hole on the cyano nitrogen that are coordinated with sodium [N1, Fig. 4(b)]. These two features combine to form a barely resolved double peak in the theoretical NEXAFS spectrum. The peak at 398.4 eV originates from excitation into LUMO+1 from both the N1 and N2 nitrogen. Finally, the peak at 399.6 eV mainly consists of contributions from excitations into LUMO+3 and LUMO+4 from the N2 nitrogen.

The C *K*-edge NEXAFS spectra of $V(\text{TCNE})_x$ and fully Na-doped TCNE are depicted in Fig. 6(a). We see that both spectra feature a weak absorption peak at ~ 284 eV. The structures at higher photon energies deviate, however, as the feature at 285.2 eV in the NaTCNE spectrum is absent for $V(\text{TCNE})_x$ and the $V(\text{TCNE})_x$ peaks are significantly broader. The N *K*-edge NEXAFS spectra show similar features at roughly the same energies, but the peaks and shoulders of the $V(\text{TCNE})_x$ spectrum are slightly more broadened and the relative intensity of the absorption onset is higher for Na-doped TCNE, see Fig. 6(b).

DISCUSSION

The core level spectroscopy shows that the alkali-intercalated TCNE system models the valency of the TCNE in $V(\text{TCNE})_x$ well, i.e., TCNE^- . However, as the ultraviolet photoelectron spectroscopy shows, the frontier occupied electronic structure differs as the covalent bonding between vanadium and the cyano-nitrogen in $V(\text{TCNE})_x$ introduces hybridization,^{9,12} whereas the SOMO of the NaTCNE system is located solely on the TCNE. The theoretical NEXAFS spectra of pristine TCNE show excellent agreement with the experimental results. The N *K*-edge spectrum offers the best agreement, probably due to the effect of the carbon-dip in C *K*-edge spectrum that is hard to completely avoid even by background subtraction. Based on the theory, we can assign the onset absorption peak in both spectra to excitation into the LUMO of TCNE.

Na doping of TCNE leads to the creation of a SOMO as the former TCNE LUMO is occupied by one electron donated from the sodium. The NEXAFS C and N *K*-edge spectra are modified upon doping, with the absorption onset peak being drastically reduced in its relative intensity for both edges as compared to pristine TCNE. This effect is reproduced by the theoretical NEXAFS spectra and is explained by the population of the former LUMO, creating the SOMO and thus reducing the available density of states by half for the absorption onset. The agreement between experiment and theory is again rather good for the N *K* edge, but for the C *K*

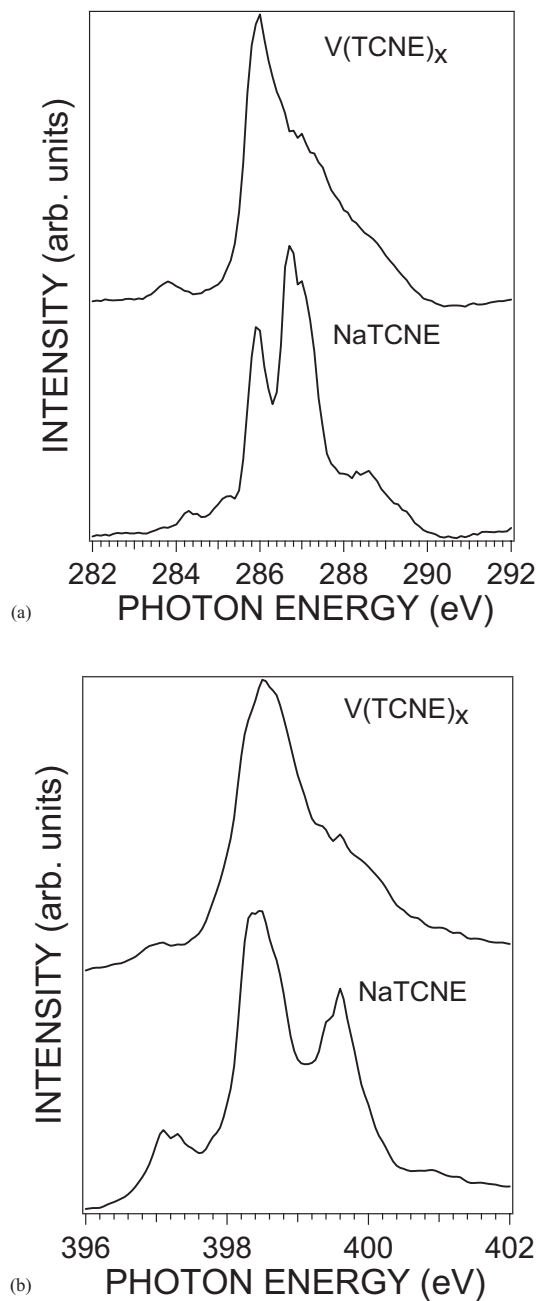


FIG. 6. (a) The C *K*-edge NEXAFS spectra of $V(\text{TCNE})_x$ and fully Na-doped TCNE. (b) The N *K*-edge NEXAFS spectra of $V(\text{TCNE})_x$ and fully Na-doped TCNE.

edge the agreement at the higher photon energy absorption events is less impressive and the reason for this is not clear. This discrepancy could in part be explained by the problem of compensating for the carbon dip, but the position of the sodium ion may also play a role. Two different Na positions were tried as well as calculating the NEXAFS spectra of TCNE^- without a counter ion present. Varying the position did not produce large differences, though the absence of a counter ion did. However, it may be the geometry that produced the best fit in our calculations (shown in the figures) is not the optimal one and contributes to the poor fit of the C *K*-edge spectra. Finally, it has been shown in previous calcu-

lations that the transition energies of TCNE can be strongly modified by very small changes in the ground state geometry,²⁰ and it may be that the calculated bond lengths and angles for the vinyl bridge are slightly off whereas the cyano groups are better described. Comparing our vinyl bond length for the Na⁺-compensated TCNE anion, 1.448 Å, with results from literature on TCNE anions, 1.420–1.429 Å (Ref. 21) and 1.44–1.443 Å,¹⁹ we see that our bond lengths are slightly longer. The vinyl-cyano carbon-carbon bond length in our calculations, 1.403–1.412 Å, is in line with one report, 1.406–1.417 Å,²¹ and slightly shorter than the range found in another study, 1.416–1.431 Å.¹⁹ As the exact reason for the C *K*-edge deviations between the experimental and theoretical spectra at higher photon energy is unclear, we cannot with certainty trace the origin of the absorption peaks. The good agreement of the N *K*-edge spectra, however, gives reason to assign the higher photon energy absorption features according to the calculated results.

The comparison between the NEXAFS C and N *K*-edge spectra of V(TCNE)_x and NaTCNE yields a qualitative agreement for both absorption edges. Interestingly, the agreement is significantly better for the N *K*-edge case, with all peaks reproduced at the same energies, with differences only in the width of the high photon energy features (a broad shoulder 399.6 eV rather than a resolved peak) and the relative intensity of the absorption onset that is slightly lower as compared to the main peak for V(TCNE)_x. This suggests that the NaTCNE model system does a good job in describing the nitrogen-based frontier unoccupied electronic structure of V(TCNE)_x and that both the charge and geometry of the cyano groups are similar for the two systems. Specifically, this suggests that the lowest unoccupied molecular orbital with density on the nitrogen atoms in V(TCNE)_x has no significant hybridization with vanadium, in contrast to the HOMO of V(TCNE)_x.^{9,12}

In the C *K*-edge spectrum, however, the absence of the peak at ~285.2 eV, reversed relative intensity of the two main absorption peaks as well as significant broadening at high energies, suggest that geometry of vinyl backbone of TCNE and its connecting bonds to the cyano groups are quite different from that for V(TCNE)_x compared to NaTCNE. The reason for this discrepancy is likely found in the differing film morphology of the two systems. The Na-doped TCNE films are amorphous and consist of NaTCNE complexes when fully doped. The V(TCNE)_x films are amorphous and known to form networks where each vanadium is coordinated to six nitrogen (and hence cyano groups) with near identical V-N bond lengths.¹⁰ Though the exact structure is not known, it is likely that the strong local coordination between the vanadium and the cyano groups will introduce both some twisting and stretching to the vinyl units to compensate, which as previously has been shown can introduce strong modification to the transition energies of TCNE.²⁰

Despite the failure of the C *K*-edge spectrum of NaTCNE to precisely model the V(TCNE)_x spectrum, we speculate that the carbon-based frontier unoccupied molecular orbital of V(TCNE)_x also has no significant hybridization with va-

niadium. We base the speculation on the nature of the TCNE anion SOMO that is delocalized over the whole TCNE molecule, i.e., nitrogen and carbon atoms share the same lowest unoccupied molecular orbital. The N-*K* edge spectra comparison show that the lowest unoccupied molecular orbital with density on the nitrogen atoms in V(TCNE)_x is NaTCNE-like, i.e., similar to the (shared) SOMO and not significantly hybridized with vanadium. Thus the onset of absorption in the C *K*-edge spectrum of V(TCNE)_x should also originate from excitation into the same, nonhybridized molecular orbital.

SUMMARY AND CONCLUSIONS

We have studied TCNE upon sodium doping with PES and NEXAFS as well as with theoretical calculations. We have used the sodium-intercalated TCNE as a model system of the more complex organic-based magnet V(TCNE)_x in order to interpret its C and N *K*-edge NEXAFS spectra and in so doing shed light on the frontier unoccupied electronic structure of V(TCNE)_x. For completely sodium-doped TCNE, one electron is donated to each TCNE molecule and the C- and N-*K*-edge NEXAFS spectra are strongly modified compared to the pristine case caused by partial filling of the TCNE LUMO. Comparing the N *K*-edge spectra of NaTCNE and V(TCNE)_x we conclude that the sodium-doped system models the nitrogen-based frontier unoccupied electron structure of V(TCNE)_x well and that the lowest unoccupied molecular orbital with density on the nitrogen atoms in V(TCNE)_x has no significant hybridization with vanadium and is similar to the SOMO of the TCNE anion, in contrast to the HOMO of V(TCNE)_x that show strong hybridization with vanadium.^{9,12} We further speculate that the carbon-based frontier unoccupied molecular orbital of V(TCNE)_x also has no significant hybridization with vanadium and that it is the same (shared) molecular orbital as the one responsible for the absorption onset in the N *K*-edge spectrum. Our results hence suggest that the LUMO of V(TCNE)_x is either localized on the TCNE ligands or on the V atoms, which is in partial agreement with the prediction that the LUMO is located on the TCNE anion.²⁴ The radically different nature of the occupied and unoccupied frontier orbitals in V(TCNE)_x will likely affect both charge injection and transport in the system.

ACKNOWLEDGMENTS

The authors acknowledge financial support from the Swedish Research Council (VR), the Carl Tryggers Foundation, and the Swedish Foundation for Strategic Research funded Center for Advanced Molecular Materials (CAMM). Z. Y. Wu acknowledges the financial support of the Outstanding Youth Fund (Grant No. 10125523), the Key Important Nano Research Project (Grant No. 90206032) of the National Natural Science Foundation of China and the Knowledge Innovation Program of the Chinese Academy of Sciences (Grant No. KJCX2-SW-N11).

- ¹S. A. Wolf, D. D. Awschalom, R. A. Buhrman, J. M. Daughton, S. V. Molnár, M. L. Roukes, A. Y. Chtelkanova, and D. M. Treger, *Science* **294**, 1488 (2001).
- ²S. A. Wolf and D. Treger, *IEEE Trans. Magn.* **36**, 2748 (2000).
- ³*Magnetic Nanostructures*, edited by H. S. Nalwa (American Scientific Publishers, Los Angeles, 2002), pp. 359–405.
- ⁴J. M. Manriquez, G. T. Yee, R. S. McLean, A. J. Epstein, and J. S. Miller, *Science* **252**, 1415 (1991).
- ⁵C. M. Wynn, M. A. Girtu, J. Zhang, J. S. Miller, and A. J. Epstein, *Phys. Rev. B* **58**, 8508 (1998).
- ⁶M. A. Girtu, C. M. Wynn, J. Zhang, J. S. Miller, and A. J. Epstein, *Phys. Rev. B* **61**, 492 (2000).
- ⁷J. S. Miller, *Inorg. Chem.* **39**, 4392 (2000).
- ⁸K. I. Pokhodnya, D. Pejakovic, A. J. Epstein, and J. S. Miller, *Phys. Rev. B* **63**, 174408 (2001).
- ⁹C. Tengstedt, M. P. de Jong, A. Kanciurzevska, E. Carlegrim, and M. Fahlman, *Phys. Rev. Lett.* **96**, 057209 (2006).
- ¹⁰D. Haskel, Z. Islam, J. Lang, C. Kmety, G. Srajer, K. I. Pokhodnya, A. J. Epstein, and J. S. Miller, *Phys. Rev. B* **70**, 054422 (2004).
- ¹¹C. Tengstedt, M. Unge, M. P. de Jong, S. Stafström, W. R. Salaneck, and M. Fahlman, *Phys. Rev. B* **69**, 165208 (2004).
- ¹²M. P. de Jong, C. Tengstedt, A. Kanciurzevska, E. Carlegrim, W. R. Salaneck, and M. Fahlman, *Phys. Rev. B* **75**, 064407 (2007).
- ¹³M. A. Reed, C. Zhou, C. J. Muller, T. P. Burgin, and J. M. Tour, *Science* **278**, 252 (1997).
- ¹⁴Y. Luo, C.-K. Wang, and Y. Fu, *Chem. Phys. Lett.* **369**, 299 (2003).
- ¹⁵G. Iucci, K. Xing, M. Lögdlund, M. Fahlman, and W. R. Salaneck, *Chem. Phys. Lett.* **244**, 139 (1995).
- ¹⁶M. Fahlman, P. Bröms, D. A. dos Santos, S. C. Moratti, N. Johansson, K. Xing, R. Friend, A. B. Holmes, J. L. Brédas, and W. R. Salaneck, *J. Chem. Phys.* **102**, 8167 (1995).
- ¹⁷J. L. Brédas, J. Cornil, and A. J. Heeger, *Adv. Mater. (Weinheim, Ger.)* **8**, 447 (1996).
- ¹⁸N. Johansson, D. A. dos Santos, S. Guo, J. Cornil, M. Fahlman, J. Salbeck, H. Schenk, H. Arwin, J. L. Brédas, and W. R. Salaneck, *J. Chem. Phys.* **107**, 2542 (1997).
- ¹⁹B. Milián, R. Pou-Amérigo, R. Viruela, and E. Ortí, *Chem. Phys. Lett.* **375**, 376 (2003).
- ²⁰I. García-Cuesta, A. M. J. Sánchez de Méras, and H. Koch, *J. Chem. Phys.* **118**, 8216 (2003).
- ²¹B. Milián, R. Pou-Amérigo, M. Merchán, and E. Ortí, *ChemPhysChem* **6**, 503 (2005).
- ²²P. W. Langhoff, *Electron-Molecule and Photon-Molecule Collisions* (Plenum, New York, 1979).
- ²³P. W. Langhoff, *Theory and Application of Moment Methods in Many-Fermion Systems* (Plenum, New York, 1980).
- ²⁴V. N. Prigodin, N. P. Raju, K. I. Pokhodnya, J. S. Miller, and A. J. Epstein, *Synth. Met.* **135-136**, 87 (2003).